Kinetic Isotope Effects in Multipath VTST. Application to a Hydrogen Abstraction Reaction

Luis Simón-Carballido,[†] Tiago Vinicius Alves,[‡] Agnieszka Dybala-Defratyka,[¶] and Antonio Fernández-Ramos[*,†]

Department of Physical Chemistry and Center for Research in Biological Chemistry and Molecular Materials (CIQUS), University of Santiago de Compostela, 15782 Santiago de Compostela, Spain, Departamento de Química Fundamental, Instituto de Química, Universidade de São Paulo, Av. Prof. Lineu Prestes 748, São Paulo, SP, 05508-000, Brazil, and Institute of Applied Radiation Chemistry, Faculty of Chemistry, Lodz University of Technology, Zeromskiego 116, Lodz, Poland.

E-mail: qf.ramos@usc.es

Abstract

In this work we apply multipath canonical variational transition state theory with small-tunneling corrections (MP-CVT/SCT) to the hydrogen abstraction reaction from ethanol by atomic hydrogen in aqueous solution at room temperature. This reaction presents two transition states which can interconvert by internal rotations about single bonds and another two transition states that are non interconvertible enantiomers to the former structures. The study also includes another three reactions with isotopically substituted species for which there are experimental values of thermal rate constants

[*]To whom correspondence should be addressed
[†]Universidade de Santiago de Compostela
[‡]Universidade de São Paulo
[¶]Lodz University of Technology

and kinetic isotope effects (KIEs). The agreement between the MP-CVT/SCT thermal rate constants and the experimental data is good. The KIEs obtained by the MP-CVT/SCT methodology are factorized in terms of individual transition state contributions to facilitate the analysis. It was found that the percentage contribution of each transition state to the total KIE is independent of the isotopic substitution.

1 Introduction

Variational transition state theory (VTST),[1–3] a much improved version of conventional transition state theory (TST),[4] is one of the most applied and successful methodologies to calculate thermal rate constants and kinetic isotope effects (KIEs).[5] Although, VTST has been mostly used to study gas-phase reactions, it can also deal with reactions in solution,[6] enzyme catalysis[7] and gas-surface reactions.[8]

TST assumes that the molecules that cross the dividing surface, which is located at the transition state (the bottleneck for reaction), never return to reactants.[9] In the canonical version of VTST this approximation is smothered by allowing the dividing surface to move along a given path. The location of the dividing surface is the one that maximizes the free energy. A maximum in the free energy along a given reaction path is a minimum in the forward flux toward products, so the CVT rate constant is always smaller or equal to its TST counterpart.[10] In most cases, this search is carried out along dividing surfaces orthogonal to the minimum energy path (MEP),[11] and each of the locations of the dividing surface defines a generalized transition state, being the one that maximizes the free energy the variational transition state.[12] On the other hand, VTST also incorporates quantum effects (mainly tunneling),[13,14] so it can deal with proton transfer reactions at low temperatures.

A recent extension of VTST, called multipath VTST (MP-VTST),[15,16] is designed to calculate thermal rate constants in flexible molecules with multiple conformations. In those cases, all the conformations of reactants can be reached by internal rotations about single bonds, and it is assumed that the interconversion barriers between conformers are smaller than the barriers for reaction. One interesting alternative to VTST for hydrogen transfer reactions in which tunneling effects are important is instanton theory.[17–19] However, in a case with multiple transition states, we prefer to use a methodology which can easily incorporate this feature. Therefore, in this work we apply MP-VTST to calculate the thermal rate constant of the hydrogen abstraction reaction from ethanol by atomic hydrogen in aqueous solution at room temperature:

$$H + CH_3CH_2OH \longrightarrow H_2 + CH_3CHOH \qquad (R1)$$

The molecule of ethanol presents three different conformations as shown in Scheme 1. The hydrogen of the -OH group can be oriented in gauche (g^+ and g^-) or in trans (t) configurations with respect to the methyl group. These conformations can be reached by internal rotations with barriers which are much lower than the barrier for reaction.

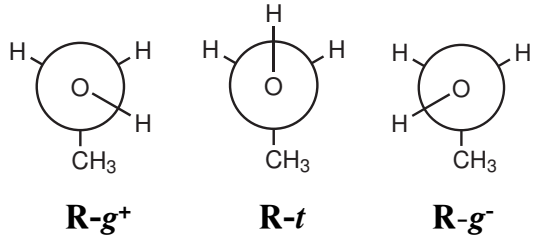

Scheme 1: Conformations of ethanol.

Recently, one of us studied reaction R1 and the H-abstraction from the methyl and $-$OH groups in gas-phase in a wide range of temperatures.[20] It was found that below $T = 500$ K only R1 contributes to the total rate constant. However, the H-abstraction from a hydrogen atom bonded to the secondary carbon leads to a reaction channel with two transition states as indicated in Scheme 2.

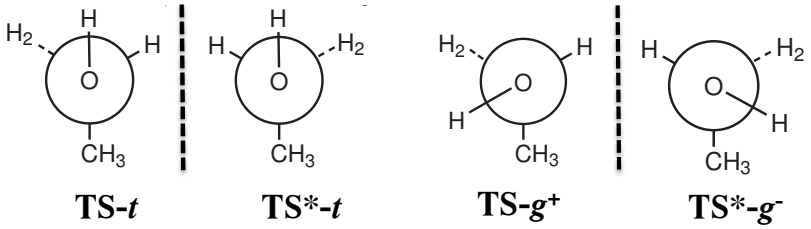

Scheme 2: Transition state conformations. The structures on both sides of the vertical line are enantiomers. H_2 indicates the hydrogen being abstracted.

In structures TS-g^+ and TS-t the methyl group is in gauche and trans dispositions, respectively, with respect to the -OH group. Both transition states can interconvert between them by internal rotation about the C-O bond. Obviously, there are two additional transition

states (TS*-g^- and TS*-t) when the other hydrogen is abstracted. Transition state with the TS-g^- or TS*-g^+ configurations were not found in the potential energy surface. Because there are more than one transition state, it is interesting to calculate the contribution of each of the transition states to the total reaction and to analyze how this percentage changes with isotope substitutions. This is the goal of this work. Specifically, we study the following reactions:

$$H + CD_3CD_2OH \longrightarrow HD + CD_3CDOH \quad \text{(R2)}$$

$$D + CH_3CH_2OD \longrightarrow DH + CH_3CHOD \quad \text{(R3)}$$

$$D + CD_3CD_2OD \longrightarrow D_2 + CD_3CDOD \quad \text{(R4)}$$

Room temperature thermal rate constants in aqueous solution have been measured by Roduner and Bartels[21] (reactions R1 and R2) and by Lossack et al.[22] (reactions R3 and R4), who found relatively high kinetic isotope effects (KIEs) with values of 7.4 and 6.4 for the ratios R1/R2 and R1/R4, respectively, whereas the ratio R1/R3 leads to an inverse KIE of 0.73. These data show important differences in the magnitude of KIEs depending on which atoms are deuterated. In this work, we also carry out an analysis of each of the contributions in which the KIE is partitioned to clarify this issue. Our partition of the KIEs has some similarities to the work of Pernía and Williams,[23] but the procedure we describe in Section 2 is based on MP-VTST, and no ensemble averages are performed. For the above reactions there is a small number of transition state structures and the solvent is treated by a continuum model instead of performing molecular dynamics simulations, so it is possible to analyze in detail the contributions to the KIE of each individual transition state.

Section 2 briefly describes the MP-VTST methodology and how to factorize the KIE in order to gain insight into the reaction mechanism. Section 3 contains computational details. Section 4 presents the application of the described methodology to reactions R1 to R4. Section 5 concludes.

2 Methodology

The calculation of thermal rate constants in solution using VTST can be carried out by different approaches. Here we employ the equilibrium solvation path approximation (ESP)[24] in which the reaction path is calculated over the potential of mean force:

$$W(\mathbf{R},T) = V(\mathbf{R}) + \Delta G^{\circ}_{\mathrm{S}}(\mathbf{R},T) \tag{1}$$

where $V(\mathbf{R})$ is the potential energy in the gas-phase, $\mathbf{R}$ being the coordinates of the solute and $\Delta G^{\circ}_{\mathrm{S}}(\mathbf{R},T)$ is the standard-state free energy of solvation. The solution-phase standard-state free energy $G^{\circ}(\mathbf{R},T)$ at a given structure $\mathbf{R}$ is given by:

$$G^{\circ}(\mathbf{R},T) = W(\mathbf{R},T) + G_{\mathrm{RVE}}(\mathbf{R},T) \tag{2}$$

where $G_{\mathrm{RVE}}(\mathbf{R},T)$ is the rovibrational free energy of structure $\mathbf{R}$, which hereafter will be written as a function of the rovibrational partition functions. In the ESP approximation the bottleneck for reaction is located at the value of the reaction coordinate that maximizes the free energy of activation calculated from Eq. 2. The solvent molecules are treated by using the canonical-mean-shape (CMS) potential,[25] $U(\mathbf{R},T)$, which in the zero-order approximation (CMS-0) is given by:

$$U(\mathbf{R},T) = W(\mathbf{R},T) \tag{3}$$

In this context the VTST calculations carried out in the gas-phase and in solution within the ESP approximation are quite similar in the sense that in the former the potential energy along the MEP is substituted by the potential of Eq. 3. The same type of modification is incorporated to the ground-state vibrationally adiabatic potential in the evaluation of quantum effects.

If the bottleneck for reaction is located at the transition state and variational and quantum effects are negligible, the thermal rate constants can be evaluated using conventional

transition state theory (TST) which only needs information of the reactants (R) and the transition state (‡), and is given by

$$k^{\mathrm{TST}}(T) = B(T)\frac{Q^{\ddagger}_{\mathrm{rot}}Q^{\ddagger}_{\mathrm{vib}}}{Q_{\mathrm{rot,R}}Q_{\mathrm{vib,R}}} \tag{4}$$

Q_{rot} and Q_{vib} are the rotational and vibrational partition functions. The latter is calculated using as reference the bottom of the well. The factor $B(T)$ is given by:

$$B(T) = \frac{1}{h\beta}\frac{Q^{\ddagger}_{\mathrm{e}}}{Q_{\mathrm{e,R}}}\frac{1}{\Phi_{\mathrm{rel}}}e^{-\beta U^{\ddagger}_0} \tag{5}$$

It is a coefficient which includes the electronic partition functions (Q_e) of the transition state and of the reactants; the partition function including the relative translational motion of the reactants, Φ_{rel}, which is the unity for unimolecular reactions; and the difference in the CMS-0 potential, $U^{\ddagger}_0$, between the reactants and the transition state. If both variational and quantum effects are of importance, canonical variational transition state theory with multidimensional corrections for tunneling (CVT/MT) should be used. The relation between TST and CVT is through a multiplicative transmission coefficient, $\gamma^{\mathrm{CVT/MT}}$, i.e.,

$$k^{\mathrm{CVT/MT}}(T) = \gamma^{\mathrm{CVT/MT}}(T)k^{\mathrm{TST}}(T) \tag{6}$$

and

$$\gamma^{\mathrm{CVT/MT}}(T) = \Gamma^{\mathrm{CVT}}(T)\kappa^{\mathrm{CVT/MT}}(T) \tag{7}$$

where $\Gamma^{\mathrm{CVT}}(T)$ and $\kappa^{\mathrm{CVT/MT}}(T)$ incorporate variational and quantum effects, respectively.

If we label the rate constants for the hydrogen and deuterium transfer reactions as $k^{\mathrm{CVT/MT}}_{\mathrm{H}}(T)$ and $k^{\mathrm{CVT/MT}}_{\mathrm{D}}(T)$, then the KIE, $\eta(T)$, is given by the ratio:

$$\eta(T) = \frac{k^{\mathrm{CVT/MT}}_{\mathrm{H}}(T)}{k^{\mathrm{CVT/MT}}_{\mathrm{D}}(T)} \tag{8}$$

It is possible to factorize the total KIE into the following contributions:

$$\eta = \eta_{\text{trans}} \eta_{\text{rv}}^{\ddagger} \eta_{\text{vtun}} \tag{9}$$

where η_{trans} is the translational contribution to KIE

$$\eta_{\text{trans}} = \frac{\Phi_{\text{rel,D}}}{\Phi_{\text{rel,H}}} \tag{10}$$

The TST rovibrational contribution to KIE is given by:

$$\eta_{\text{rv}}^{\ddagger} = \frac{Q_{\text{R,D}}}{Q_{\text{R,H}}} \frac{Q_{\text{rot,H}}^{\ddagger} Q_{\text{vib,H}}^{\ddagger}}{Q_{\text{rot,R,D}} Q_{\text{vib,R,D}}} \tag{11}$$

and the variational and tunneling contributions by:

$$\eta_{\text{vtun}} = \frac{\gamma_{\text{H}}^{\text{CVT/MT}}}{\gamma_{\text{D}}^{\text{CVT/MT}}} \tag{12}$$

In flexible molecules it is possible to have more than one transition state for a given reaction channel k. The set of all the $n_k^{\ddagger}$ transition states which can be reached by internal rotations about single bonds is called conformational reaction channel (CRC). If there are K CRCs (with $k = 1, \ldots, K$), the total number of transition states is $n^{\ddagger} = n_1^{\ddagger} + \ldots + n_K^{\ddagger}$. If the reactants are also flexible and have several conformations n_{R} with interconversion barriers between conformers lower than the barrier to reach the most stable transition state, all conformers from reactants contribute to any of the transition states $n^{\ddagger}$. The total rate constant evaluated by TST is a multipath rate constant and it is a sum over all of the CRCs of interest. Multipath TST can also include anharmonic effects due to the hindered rotations,[26–29] which in the two-dimensional nonseparable approximation[30] are included as

a multiplicative coefficient, $\alpha_{\mathrm{tor},k}$, to the harmonic rate constant:

$$k^{\mathrm{MP-TST}}(T) = \sum_{k=1}^{K} \alpha_{\mathrm{tor},k} \tilde{k}^{\mathrm{TST}}_{\mathrm{har},k}(T) \tag{13}$$

and is given by

$$\alpha_{\mathrm{tor},k} = \frac{\alpha^{\ddagger}_{\mathrm{tor}}}{\alpha_{\mathrm{tor,R}}} \tag{14}$$

and $\alpha^{\ddagger}_{\mathrm{tor},k}$ and $\alpha_{\mathrm{tor,R}}$ are the anharmonic corrections at the TSs of the kth CRC and of reactants, respectively. The harmonic TST thermal rate constant of a given CRC is given by:

$$\tilde{k}^{\mathrm{TST}}_{\mathrm{har},k}(T) = B(T) e^{-\beta W^{\ddagger}_{k}} \frac{\tilde{Q}^{\ddagger}_{\mathrm{har},k}}{\tilde{Q}_{\mathrm{har,R}}}, \tag{15}$$

where $W^{\ddagger}_{k}$ is the difference in energy between the lowest energy transition state and the lowest energy transition state of the k-th CRC. The multi-conformational partition function of reactants is given by:

$$\tilde{Q}_{\mathrm{har,R}} = \sum_{j}^{n_{\mathrm{R}}} Q^{\mathrm{RRHO}}_{j,\mathrm{R}} \tag{16}$$

where

$$Q^{\mathrm{RRHO}}_{j,\mathrm{R}} = Q_{\mathrm{rot,j,R}} Q_{\mathrm{vib,j,R}} e^{-\beta U_j} \tag{17}$$

and U_j is the difference in energy between the lowest conformation of reactants and conformation j. Similarly, for the transition states

$$\tilde{Q}^{\ddagger}_{\mathrm{har},k} = \sum_{i_k=1}^{n^{\ddagger}_{k}} Q^{\mathrm{RRHO},\ddagger}_{i_k} \tag{18}$$

and

$$Q^{\mathrm{RRHO},\ddagger}_{i_k} = Q^{\ddagger}_{\mathrm{rot},i_k} Q^{\mathrm{HO},\ddagger}_{i_k} e^{-\beta U^{\ddagger}_{i_k}} \tag{19}$$

where $Q^{\ddagger}_{\mathrm{rot},i_k}$ and $Q^{\mathrm{HO},\ddagger}_{i_k}$ are rotational and vibrational partition functions, respectively, of each of the individual transition states ($i_k = 1, \ldots, n^{\ddagger}_{k}$) that belong to the k-th CRC. The

barrier $U_{i_k^\ddagger}$ refers to the difference in energy between the lowest energy transition state and transition state i_k within the same CRC. The TST rate constant due to transition state i_k is given by

$$k^{\mathrm{TST}}_{\mathrm{har},i_k}(T) = B(T)e^{-\beta W_k^\ddagger}\frac{Q^{\mathrm{RRHO},\ddagger}_{i_k}}{\tilde{Q}_{\mathrm{har,R}}} \tag{20}$$

and

$$\tilde{k}^{\mathrm{TST}}_{\mathrm{har},k}(T) = \sum_{i_k=1}^{n_k^\ddagger} k^{\mathrm{TST}}_{\mathrm{har},i_k}(T) \tag{21}$$

Quantum effects and recrossing are both incorporated in CVT/MT, as in Eq. 6, through a multiplicative coefficient $\gamma^{\mathrm{CVT/MT}}_{i_k}$ to each of the transition states, i.e.,

$$k^{\mathrm{CVT/MT}}_{\mathrm{har},i_k} = \gamma^{\mathrm{CVT/MT}}_{i_k} k^{\mathrm{TST}}_{\mathrm{har},i_k}(T) \tag{22}$$

where

$$\gamma^{\mathrm{CVT/MT}}_{i_k} = \Gamma^{\mathrm{CVT}}_{i_k}\kappa^{\mathrm{CVT/MT}}_{i_k}, \tag{23}$$

The recrossing is given by:

$$\Gamma^{\mathrm{CVT}}_{i_k} = \frac{k^{\mathrm{CVT}}_{\mathrm{har},i_k}}{k^{\mathrm{TST}}_{\mathrm{har},i_k}} \tag{24}$$

and the quantum effects evaluated by the multidimensional semiclassical approximation MT, are incorporated through the transmission coefficient $\kappa^{\mathrm{CVT/MT}}_{i_k}$. The multipath CVT/MT rate constant is given by:

$$k^{\mathrm{MP-CVT/MT}}(T) = \sum_{k=1}^{K} \alpha_{\mathrm{tor},k}\tilde{k}^{\mathrm{CVT/MT}}_{\mathrm{har},k}(T) \tag{25}$$

To simplify the notation, let's assume that there is only one CRC, i.e., $K = 1$, although the following equations can be extended to any number of CRC's. The KIE due to a given isotopically substituted species is obtained from the ratio:

$$\eta^{\mathrm{MP-CVT/MT}} = \frac{k^{\mathrm{MP-CVT/MT}}_{\mathrm{H}}}{k^{\mathrm{MP-CVT/MT}}_{\mathrm{D}}} \tag{26}$$

where $k_{\mathrm{H}}^{\mathrm{MP-CVT/MT}}$ and $k_{\mathrm{D}}^{\mathrm{MP-CVT/MT}}$ are the MP-CVT/MT thermal rate constants for the root and isotopically substituted species, respectively. For the case of one CRC, the ratio of Eq. 26 coincides with the ratio:

$$\tilde{\eta} = \frac{\tilde{k}_{\mathrm{H}}^{\mathrm{CVT/MT}}}{\tilde{k}_{\mathrm{D}}^{\mathrm{CVT/MT}}} \tag{27}$$

Multiplying and dividing the above expression by $k_{i,\mathrm{D}}^{\mathrm{CVT/MT}}$ and rearranging the terms, the following expression is obtained:

$$\tilde{\eta} = \eta_{\mathrm{tor}} \sum_{i}^{n^{\ddagger}} P_{i,\mathrm{D}} \eta_i \tag{28}$$

where the anharmonic contribution to the KIE is given by the ratio:

$$\eta_{\mathrm{tor}} = \frac{\alpha_{\mathrm{tor,H}}}{\alpha_{\mathrm{tor,D}}} \tag{29}$$

The contributions to η_i, which is the KIE due to the ith TS,

$$\eta_i = \frac{k_{i,\mathrm{H}}^{\mathrm{CVT/MT}}}{k_{i,\mathrm{D}}^{\mathrm{CVT/MT}}} \tag{30}$$

are factorized in the same terms as Eq. 9 plus the anharmonic contribution:

$$\eta = \eta_{\mathrm{tor}} \eta_{\mathrm{trans}} \eta_{\mathrm{rv}}^{\ddagger} \eta_{\mathrm{vtun}} \tag{31}$$

However, in this case the rovibrational contribution to the KIE involves multiconformational partition functions of reactants, i.e.,

$$\eta_{i,\mathrm{rv}}^{\ddagger} = \frac{\tilde{Q}_{\mathrm{har,R,D}}}{\tilde{Q}_{\mathrm{har,R,H}}} \frac{Q_{i,\mathrm{H}}^{\mathrm{RRHO},\ddagger}}{Q_{i,\mathrm{D}}^{\mathrm{RRHO},\ddagger}} \tag{32}$$

The coefficient $P_{i,\mathrm{D}}$ is the ratio between the individual and total rate constants of the iso-

topically substituted species, i.e.,

$$P_{i,\mathrm{D}} = \frac{k_{i,\mathrm{D}}^{\mathrm{CVT/MT}}}{\tilde{k}_{\mathrm{D}}^{\mathrm{CVT/MT}}} \tag{33}$$

It can be rewritten as:

$$P_{i,\mathrm{D}} = \frac{\gamma_{i,\mathrm{D}}^{\mathrm{CVT/MT}} Q_{i,\mathrm{D}}^{\mathrm{RRHO},\ddagger}}{\sum_i^{n^\ddagger} \gamma_{i,\mathrm{D}}^{\mathrm{CVT/MT}} Q_{i,\mathrm{D}}^{\mathrm{RRHO},\ddagger}} \tag{34}$$

If we define the weighted individual KIE as

$$\tilde{\eta}_i = P_{i,\mathrm{D}} \eta_i, \tag{35}$$

the total KIE is given by:

$$\tilde{\eta} = \sum_i^{n^\ddagger} \tilde{\eta}_i \tag{36}$$

It is also interesting to calculate the ratio between the weighted individual KIE and the total KIE, which it leads to:

$$P_{i,\mathrm{H}} = \frac{\tilde{\eta}_i}{\tilde{\eta}} = \frac{\gamma_{i,\mathrm{H}}^{\mathrm{CVT/MT}} Q_{i,\mathrm{H}}^{\mathrm{RRHO},\ddagger}}{\sum_i^{n^\ddagger} \gamma_{i,\mathrm{H}}^{\mathrm{CVT/MT}} Q_{i,\mathrm{H}}^{\mathrm{RRHO},\ddagger}} \tag{37}$$

Eq. 37 provides the contribution of each TS to the total KIE. The result is invariant on the isotopic substitution, depending only on the characteristics of the transition states. This equation is further discussed in Section 4.

3 Computational details

Solvent effects were incorporated by using the PCM model[31] together with the DFT electronic structure MPWB1K method,[32] with the augmented polarized double-ζ basis set, 6-31+G(d,p).[33] This level of calculation performs well for nonmetallic thermochemical data and thermochemistry.[34] The energies, optimized geometries and Hessians of the stationary points were obtained with Gaussian09.[35] The normal-mode frequencies were scaled by a factor of 0.964.[36] Very recently, it has been found that scaled frequencies give better results

than unscaled harmonic frequencies in the evaluation of KIEs.[37] The anharmonic effects due to the torsions were included through the 2D-NS approximation.[30] This method involves the construction of global two-dimensional torsional potential energy surfaces, which are built by partial optimization, as described in Ref. 20. The CMS-0 potential along the reaction path (the liquid-phase MEP) was followed using the Page-McIver algorithm[38] with a stepsize of 0.01 a_0 and Hessian calculations every 9 steps. The frequencies along the reaction path were projected using redundant internal coordinates.[39] The variational transition state theory individual thermal rate constants were evaluated using CVT together with small-curvature tunneling corrections[40,41] (CVT/SCT). These calculations were carried out with the PolyRate 9.7 program[42] and this information served as feedback to calculate the multipath thermal rate constants and the KIEs.

4 Results and discussion

Ethanol molecule and the hydrogen abstraction transition states in the continuum model of water present the same conformations as in the gas phase (Schemes 1 and 2), but as expected the barrier height for reaction is significantly reduced. Specifically, for reaction R1 the reduction is of 1.47 kcal/mol for both conformers when comparing the gas-phase MC3BB calculations with the PCM/MPWB1K/6-31+G(d,p) calculations of this work. The calculation of the harmonic MP-CVT/SCT thermal rate constants requires the evaluation of the partition function of reactants. This should include the three indistinguishable conformations of ethanol through the multiconformational partition function:

$$\tilde{Q}_{\mathrm{har,R}} = Q^{\mathrm{RRHO}}_{\mathrm{R}-t} + 2Q^{\mathrm{RRHO}}_{\mathrm{R}-g^+} \tag{38}$$

The difference in energy between the R-t and R-g^+ conformations in this case is just 0.02 kcal/mol. The last partition function of the rhs of Eq. 38 is multiplied by two because R-g^+ and R-g^- are enantiomers. The transition state multiconformational partition function of

one of the CRCs is given by:

$$\tilde{Q}^{\ddagger}_{\mathrm{har},1} = Q^{\mathrm{RRHO},\ddagger}_{\mathrm{TS}-t} + Q^{\mathrm{RRHO},\ddagger}_{\mathrm{TS}-g^{+}} \tag{39}$$

For the other CRC the multiconformational partition function of the transition state is given by:

$$\tilde{Q}^{\ddagger}_{\mathrm{har},2} = Q^{\mathrm{RRHO},\ddagger}_{\mathrm{TS}^{\star}-t} + Q^{\mathrm{RRHO},\ddagger}_{\mathrm{TS}^{\star}-g^{-}} \tag{40}$$

where TS*-t and TS*-g^{-} are the enantiomers of TS-t and TS-g^{+}, respectively, as shown in Scheme 2. The partition functions of Eqs. 39 and 40 are equal so the MP-TST thermal rate constant will be given by:

$$k^{\mathrm{MP-TST}}(T) = \tilde{k}^{\mathrm{TST}}_{\mathrm{har},1}(T) + \tilde{k}^{\mathrm{TST}}_{\mathrm{har},2}(T) = 2\tilde{k}^{\mathrm{TST}}_{\mathrm{har},1}(T) \tag{41}$$

where the factor of two takes into account the enantiomers. The energy difference between TS-t and the most stable conformation of reactants is 6.38 kcal/mol, whereas this difference increases to 6.57 in the case of TS-g^{+}. The information from Eqs. 38 and 39 together with the barrier heights allows the calculation of the multipath-TST thermal rate constants (Table 1).

Unfortunately, the MP-TST calculations produce rate constants which are too low, because they neglect quantum effects on the reaction coordinate, which are important in hydrogen transfer reactions. The MP-CVT/SCT calculations lead to larger values, closer to the experimental findings (Table 1). For reaction R1 this effect increases the MP-TST value more than three times. The magnitude of the imaginary frequencies may be also an indication of the importance of tunneling; larger values usually result in tighter reaction path potentials and, therefore, in larger tunneling contributions. Notice that in a one-dimensional potential the imaginary frequency is directly related to the curvature of the potential at the transition state (larger frequency translates into narrower potential and therefore more tun-

neling). However, the TSs of reaction R2 have smaller imaginary frequencies than the TSs of reaction R3 but larger tunneling contributions (see Table 2). The result can be understood taking into account that tunneling is a multidimensional process, so there is coupling between the reaction coordinate and the other degrees of freedom with a substantial change in the shape of the potential with respect to the one-dimensional picture. Thus, for the two transition states of reaction R2 the profiles of the ground-state vibrationally adiabatic potentials are wider than the profiles of R3 despite the magnitude of the imaginary frequency (see Fig. 1). Notice that tunneling decreases with the width of the potential. Besides, for the two TSs of R3 variational effects are quite important, which indicates that the maxima of the free energy are quite displaced from the TS structures. In the case of R3 at one point on the reactants side the formation of the C-H bond as the reaction proceeds towards reactants makes the zero-point energy to increase faster than the decrease of the CMS-0 potential, so the maximum of the ground-state vibrationally adiabatic potential appears displaced (see Fig. 1). This situation does not occur in R1 because the CMS-0 potential decreases faster than for R3, so it partially compensates the increment of the zero-point energy.

The anharmonicity due to the torsions about the C-C and C-O bonds is more important for the reactants than for the transition states as shown in Table 1. The anharmonic coefficients are larger than unity because the density of states of the torsional partition function increases faster than that of the harmonic oscillator. In any case the torsional anharmonicity slightly lowers the thermal rate constants and has no effect on the KIEs.

The different contributions to the total KIE are factorized in Table 3. Notice that in this case the KIE obtained from Eq. 26 and the one obtained from Eq. 27 are identical. The rovibrational contribution to the KIE is the one that involves the larger changes depending upon the isotopic substitution. It is close to 7 for the ratio R1/R2 and about 0.20 for R1/R3. In general the rovibrational KIE is large when the abstracted hydrogen is substituted by a deuterium. This occurs because the ratio between the reactants partition functions is large (mainly due to the difference in frequency between the C-H and C-D bonds), i.e., larger

than the ratio between transition state partition functions, which, in general, is smaller than unity. This effect was also observed in the hydrogen abstraction reaction from methanol.[43] In the present study it is definititely observed for R1/R2. The effect of $\eta_{\rm vr}$ is also seen for R1/R4, however the effect is not as large (Table 3). The translational KIE is temperature independent and large when the hydrogen atom that collides with the molecule is isotopically substituted by a deuterium (R1/R3 and R1/R4 cases), because of the increase in the reduced mass of the two particle system. The contribution of tunneling to the KIE is not as important as in hydrogen abstraction reactions in which the donor and the acceptor are heavy atoms, and the most probable path is quite far from the MEP. An increase of the transferred particle from hydrogen to deuterium has an important impact in the magnitude of the transmission coefficients for tunneling. For reactions R1 to R4 the acceptor is not a heavy atom, so the tunneling path is closer to the MEP than in a heavy-light-heavy system and therefore the contribution of tunneling to the KIE is smaller. The only exception is the R1/R3 KIE, but in this case the larger value of $\eta_{\rm vtun}$ is due to the presence of variational effects for reaction R3. With the exception of the ratio R1/R2 there are some discrepancies between the calculated and experimental KIEs. They may be related to the fact that specific solvation was not included in the description of the processes and, therefore, the coupling between explicit water molecules and the reactive species has been neglected.

Table 3 also list the contribution of each of the two transition states to the KIE. Eq. 37 shows that the weighted contribution of each individual transition state, i.e., the ratio $\tilde{\eta}_i/\tilde{\eta}$, is independent of the isotopic substitution at a given temperature. In fact, it is also independent of the characteristics of the reactants, and in this case equals 56.9% and 43.1% for all the isotopically substituted reactions occurring through the TS-t and TS-g^+ transition states, respectively. However, the ratio

$$\frac{\eta_i}{\tilde{\eta}} = \frac{P_{i,\rm H}}{P_{i,\rm D}} \tag{42}$$

is obviously not a constant, although it depends only on the characteristics of the transition state structures if TST is used. If the KIE is calculated using VTST, information along

the reaction path starting from each individual transition state is also required in order to evaluate the variational and tunneling effects. Eq. 42 shows the importance of the KIE due to an individual transition state i in the total KIE, i.e., if that particular transition state is above ($\eta_i/\tilde{\eta} > 1$) or below ($\eta_i/\tilde{\eta} < 1$) the total contribution. For instance, the transition state TS-t contributes above the total value for the KIEs R1/R2 and R1/R4 but below the average in the case R1/R3.

Notice that Eq. 37 can also be obtained from the ratio

$$P_{i,\mathrm{H}} = \frac{k_{i,\mathrm{H}}^{\mathrm{CVT/MT}}}{\tilde{k}_{\mathrm{H}}^{\mathrm{CVT/MT}}} \tag{43}$$

which is an extension of the Curtin-Hammett principle.[20,44] This principle states that the contributions of the individual transition states to the total rate constant depend exclusively on relative transition state free energies (partition functions). This principle only applies if TST assumptions are valid and usually fails when dealing with hydrogen transfer reactions due to the presence of tunneling, as in the computational study of the Swern oxidation mechanism.[45] In that work the calculated KIEs are too low when compared with experiment, which is also the case in this work if we ignore tunneling and variational effects, with KIEs of 0.53 and 3.82 for the ratios R1/R3 and R1/R4, respectively. Therefore Eq. 37 is the one to apply in cases in which we suspect tunneling and variational effects may play a role. Additionally, in this work we show that the implications of Eq. 37 go beyond the individual contributions to the thermal rate constant because it also indicates that the contribution in percentage of a given transition state to the total KIE is independent of the isotopic substitution.

5 Conclusions

In the present work we have studied the hydrogen atom abstraction from ethanol by atomic hydrogen using the MP-CVT/SCT methodology. Different isotopic substitutions within the

ethanol molecule as well as abstracting species have been considered which led to four sets of data. Within each of them, we have discussed the individual contribution of each transition state to torsional, rovibrational, translational, and tunneling KIE factors. There is a wide variety of contributing factors to the KIE depending on the isotopic substitution: R1/R2 is characterized by large rovibrational factor, small tunneling and neglegible translational contributions; R1/R4 has much smaller but not negligible rovibrational factor and substantial translational contribution; R1/R3 turned out to be unique in such respect that the rovibrational factor was very significant in the inverse sense and tunneling effect was the largest among all three studied substitutions. Overall, taking into account the quite different scenarios studied, the agreement with experiment is quite satisfactory. Additionally, we stress the importance of incorporating tunneling and variational effects into this type of reactions. We have found that in the case of several transition states that can interconvert between them, the contribution in percentage of each of them to the total KIE is invariant to the isotopic substitution.

Acknowledgments

T. V. A. thanks Fundação de Amparo à Pesquisa do Estado de São Paulo of Brazil for a post-doctoral fellowship. A. D.-D. acknowledges the SONATA-Bis research grant funded by the National Science Centre, Poland (UMO-2014/14/E/ST4/00041). A. F. R. acknowledges partial funding from Ministerio de Economia y Competitividad of Spain (Research Grant No CTQ2014-58617-R) and from Consellería de Cultura, Educación e Ordenación Universitaria of Xunta de Galicia (Research Grant No R2014/051).

References

(1) Garrett, B. C.; Truhlar, D. G. Variational Transition-State Theory. *Acc. Chem. Res.* **1980**, *13*, 440.

(2) Truhlar, D. G.; Isaacson, A. D.; Garrett, B. C. In *Theory of Chemical Reaction Dynamics*; Baer, M., Ed.; CRC: Boca Raton, FL, 1985; Vol. 4; p 65.

(3) Fernández-Ramos, A.; Ellingson, A.; Garrett, B. C.; Truhlar, D. G. Variational Transition State Theory. *Rev. Comput. Chem.* **2007**, *23*, 125.

(4) Eyring, H. The Activated Complex in Chemical Reactions. *J. Chem. Phys.* **1935**, *3*, 107–115.

(5) Garrett, B. C.; G., T. D.; Schatz, G. C. Test of Variational Transition-State Theory and Multidimensional Semiclassical Transmission Coefficient Methods Against Accurate Quantal Rate Constants for H+H_2/HD, D+H_2, and O+H_2/D_2/HD, Including Intramolecular and Intermolecular Kinetic Isotope Effects. *J. Am. Chem. Soc.* **1986**, *108*, 2876–2881.

(6) Cramer, C. J.; Truhlar, D. G. A Universal Approach to Solvation Modeling. *Acc. Chem. Res.* **2008**, *41*, 760–768.

(7) Truhlar, D. G.; Gao, J.; Garcia-Viloca, M.; Alhambra, C.; Corchado, J.; Sánchez, M. L.; Poulsen, T. D. Ensemble-Averaged Variational Transition State Theory with Optimized Multidimensional Tunneling for Enzyme Kinetics and Other Condensed-Phase Reactions. *Int. J. Quantum Chem.* **2004**, *100*, 1136–1152.

(8) Wonchoba, S. E.; Truhlar, D. G. General Potential-Energy Function for H/Ni and Dynamics Calculations of Surface Diffusion, Bulk Diffusion, Subsurface-to-Surface Transport, and Absorption. *Phys. Rev. B* **1996**, *53*, 11222–11241.

(9) Garrett, B. C. Perspective on 'The Transition State Method'. *Theor. Chem. Acc.* **2000**, *103*, 200–204.

(10) Garrett, B. C.; Truhlar, D. G. Criterion of Minimum State Density in the Transition State Theory of Bimolecular Reactions. *J. Chem. Phys.* **1979**, *70*, 1593–1598.

(11) Fukui, K. The Path of Chemical Reactions. The IRC Approach. *Acc. Chem. Research* **1981**, *14*, 363–368.

(12) Garrett, B. C.; G., T. D. Generalized Transition-State Theory. Classical Mechanical Theory and Applications to Collinear Reactions of Hydrogen Molecules. *J. Phys. Chem.* **1979**, *83*, 1052–1078.

(13) Truhlar, D. G.; Kupperman, A. Exact Tunneling Calculations. *J. Am. Chem. Soc.* **1971**, *93*, 1840–1851.

(14) Kuppermann, A. An Exact Quantum Mechanical Transition State Theory. 1. An Overview. *J. Phys. Chem.* **1979**, *83*, 171–187.

(15) Meana-Pañeda, R.; Fernández-Ramos, A. Tunneling and Conformational Flexibility Play Critical Roles in the Isomerization Mechanism of Vitamin D. *J. Am. Chem. Soc.* **2012**, *134*, 346–354; (E) **2012**, *134*, 7193.

(16) Yu, T.; Zheng, J.; Truhlar, D. G. Multi-Path Variational Transition State Theory: Rate Constant of the 1,4-Hydrogen Shift Isomerization of the 2-Cyclohexylethyl Radical. *J. Phys. Chem. A* **2012**, *116*, 297–308.

(17) Fernandez-Ramos, A.; Smedarchina, Z.; Siebrand, W.; Zgierski, M. A Direct-Dynamics Study of the Zwitterion-to-Neutral Interconversion of Glycine in Aqueous Solution. *J. Chem Phys.* **2000**, *113*, 9714–9721.

(18) Smedarchina, Z.; Siebrand, W.; Fernández-Ramos, A.; Cui, Q. Kinetic Isotope Effects for Concerted Multiple Proton Transfer: a Direct Dynamics Study of an Active-Site Model of Carbonic Anhidrase II. *J. Am. Chem. Soc.* **2003**, *125*, 243.

(19) Meisner, J.; Rommel, J. B.; Kästner, J. Kinetic Isotope Effects Calculated with the Instanton Method. *J. Comput. Chem.* **2011**, *32*, 3456–3463.

(20) Meana-Pañeda, R.; Fernández-Ramos, A. Accounting for Conformational Flexibility and Torsional Anharmonicity in the H + CH3CH2OH Hydrogen Abstraction Reactions: A Multi-Path Variational Transition State Theory Study. *J. Chem. Phys.* **2014**, *140*, 174303.

(21) Roduner, E.; Bartels, D. M. Solvent and Isotope Effects on Addition of Atomic Hydrogen to Benzene in Aqueous Solution. *Ber. Bunsenges. Phys. Chem.* **1992**, *96*, 1037–1042.

(22) Lossack, A. M.; Roduner, E.; Bartels, D. M. Kinetic Isotope Effects in H and D Abstraction Reactions from Alcohols by D Atoms in Aqueous Solution. *J. Phys. Chem. A* **1998**, *102*, 7462–7469.

(23) Ruiz-Pernía, J. J.; Williams, I. H. Ensemble-Averaged QM/MM Kinetic Isotope Effects for the SN2 Reaction of Cyanide Anion with Chloroethane in DMSO Solution. *Chem. Eur. J.* **2012**, *18*, 9405–9414.

(24) Chuang, Y.-Y.; Cramer, C. J.; Truhlar, D. G. The Interface of Electronic Structure and Dynamics for Reactions in Solution. *Int. J. Quantum Chem.* **1998**, *70*, 887–896.

(25) Truhlar, D. G.; Liu, Y.-P.; Schenter, G. K.; Garrett, B. C. Tunneling in the Presence of a Bath. A Generalized Transition-State Theory Approach. *J. Phys. Chem.* **1994**, *98*, 8396–8405.

(26) Zheng, J.; Yu, T.; Papajak, E.; Alecu, I. M.; Mielke, S. L.; Truhlar, D. G. Practical Methods for Including Torsional Anharmonicity in Thermochemical Calculations on Complex Molecules: The Internal-Coordinate Multi-Structural Approximation. *Phys. Chem. Chem. Phys.* **2011**, *13*, 10885–10907.

(27) Yu, T.; Zheng, J.; Truhlar, D. G. Multi-Structural Variational Transition State Theory. Kinetics of the 1,4-Hydrogen Shift Isomerization of the Pentyl Radical with Torsional Anharmonicity. *Chem. Sci.* **2011**, *2*, 2199–2213.

(28) Zheng, J.; Truhlar, D. G. Quantum Thermochemistry: Multistructural Method with Torsional Anharmonicity Based on a Coupled Torsional Potential. *J. Chem. Theory Comput.* **2013**, *9*, 1356–1367.

(29) Simón-Carballido, L.; Fernández-Ramos, A. Calculation of the Two-Dimensional Non-separable Partition Function for Two Molecular Systems. *J. Mol. Model.* **2014**, *20*, 2190.

(30) Fernández-Ramos, A. Accurate Treatment of Two-Dimensional Non-separable Hindered Internal Rotors. *J. Chem. Phys.* **2013**, *138*, 134112.

(31) Barone, V.; Cossi, M.; J., T. Geometry Optimization of Molecular Structures in Solution by the Polarizable Continuum Model. *J. Comp. Chem.* **1998**, *19*, 404–417.

(32) Zhao, Y.; Lynch, B. J.; Truhlar, D. G. Hybrid Meta Density Functional Theory Methods for Thermochemistry, Thermochemical Kinetics, and Noncovalent Interactions: The MPW1B95 and MPWB1K Models and Comparative Assessments for Hydrogen Bonding and van der Waals Interactions. *J. Phys. Chem A* **2004**, *108*, 6908–6918.

(33) Hehre, W. J.; Ditchfield, R.; Pople, J. A. Self-Consistent Molecular Orbital Methods. XII. Further Extensions of Gaussian-type Basis Sets for Use in Molecular Orbital Studies of Organic Molecules. *J. Chem. Phys.* **1972**, *56*, 2257–2261.

(34) Zhao, Y.; Schultz, N. E.; Truhlar, D. G. Design of Density Functionals by Combining the Method of Constant Satisfaction with Parametrization for Thermochemistry, Thermochemical Kinetics, and Noncovalent Interactions. *J. Chem. Theory Comput.* **2006**, *2*, 364–382.

(35) Frisch, M. J.; Trucks, G. W.; Schlegel, H. B.; Scuseria, G. E.; Robb, M. A.; Cheeseman, J. R.; G.Scalmani,; Barone, V.; Mennucci, B.; Petersson, G. A. *et al*. Gaussian09, Gaussian, Inc., Wallingford CT (2009).

(36) Alecu, I. M.; Zheng, J.; Zhao, Y.; Truhlar, D. G. Computational Thermochemistry: Scale Factor Databases and Scale Factors for Vibrational Frequencies Obtained from Electronic Model Chemistries. *J. Chem. Theory Comput.* **2010**, *6*, 2872–2887.

(37) Wilson, P. B.; Williams, I. H. Critical Evaluation of Anharmonic Corrections to the Equilibrium Isotope Effect for Methyl Cation Transfer from Vacuum to Dielectric Continuum. *Mol. Phys.* **2015**, *113*, 1704–1711.

(38) Page, M.; McIver Jr, J. W. On Evaluating the Reaction Path Hamiltonian. *J. Chem. Phys.* **1988**, *88*, 922–935.

(39) Chuang, Y. Y.; Truhlar, D. G. Reaction-Path Dynamics in Redundant Internal Coordinates. *J. Phys. Chem. A* **1998**, *102*, 242–247.

(40) Lu, D.-h.; Truong, T. N.; Melissas, V. S.; Lynch, G. C.; Liu, Y.-P.; Garrett, B. C.; Steckler, R.; Isaacson, A. D.; Rai, S. N.; Hancock, G. C.; Lauderdale, J. G.; Joseph, T.; Truhlar, D. G. Polyrate 4: A New Version of a Computer Program for the Calculation of Chemical Reaction Rates for Polyatomics. *Comput. Phys. Commun.* **1992**, *71*, 235.

(41) Liu, Y.-P.; Lynch, G. C.; Truong, T. N.; Lu, D.-h.; Truhlar, D. G. Molecular Modeling of the Kinetic Isotope Effect for the [1,5]-Sigmatropic Rearrangement of cis-1,3-Pentadiene. *J. Am. Chem. Soc.* **1993**, *115*, 2408–2415.

(42) Corchado, J. C.; Chuang, Y.-Y.; Fast, P. L.; Hu, W.-P.; Liu, Y.-P.; Lynch, G. C.; Nguyen, K. A.; Jackels, C. F.; Ramos, A. F.; Ellingson, B. A. *et al.* POLYRATE−version 9.7, University of Minnesota, Minneapolis (2007).

(43) Meana-Pañeda, R.; Truhlar, D. G.; Fernández-Ramos, A. High-Level Direct-Dynamics Variational Transition State Theory Calculations Including Multidimensional Tunneling of the Thermal Rate Constants, Branching Ratios, and Kinetic Isotope Effects of the Hydrogen Abstraction Reactions from Methanol by Atomic Hydrogen. *J. Chem. Phys.* **2011**, *134*, 0943202.

(44) Seeman, J. I. Effect of Conformational Change on Reactivity in Organic Chemistry. Evaluations, Applications, and Extensions of Curtin-Hammett/Winstein-Holness Kinetics. *Chem. Rev.* **1983**, *83*, 83–134.

(45) Giagou, T.; Meyer, M. P. Mechanism of the Swern Oxidation: Significant Deviations from Transition State Theory. *J. Org. Chem.* **2010**, *75*, 8088–8099.

Table 1: Room temperature multipath TST and CVT/SCT thermal rate constants (in $cm^3molecule^{-1}s^{-1}$) for reactions R1 to R4 calculated within the harmonic (har subscript) or anharmonic 2D-NS (tor subscript) approximations to treat hindered rotors. The contributions in percentage of the transition states TS-t(plus enantiomer)/TS-g^+ (plus enantiomer) to the multipath thermal rate constants. The anharmonic coefficients α for reactants (R) and transition state structures (‡).

	R1	R2	R3	R4
$k_{\rm har}^{\rm MP-TST}$	4.43×10^{-15}	6.39×10^{-16}	8.16×10^{-15}	1.16×10^{-15}
$\%{\rm TST}_i$	57.1/42.9	56.7/43.3	57.3/42.7	56.9/43.1
$k_{\rm har}^{\rm MP-CVT/SCT}$	1.46×10^{-14}	1.90×10^{-15}	1.45×10^{-14}	2.82×10^{-15}
$\%{\rm CVT/SCT}_i$	56.9/43.1	55.7/44.3	57.5/42.5	55.9/44.1
$\alpha_{\rm tor,R}$	1.291	1.283	1.264	1.256
$\alpha_{\rm tor}^{\ddagger}$	1.196	1.187	1.172	1.167
$k_{\rm tor}^{\rm MP-TST}$	4.11×10^{-15}	5.92×10^{-16}	7.56×10^{-15}	1.08×10^{-15}
$k_{\rm tor}^{\rm MP-CVT/SCT}$	1.35×10^{-14}	1.76×10^{-15}	1.35×10^{-14}	2.62×10^{-15}
$k_{\rm exp}$	3.39×10^{-14} [a]	4.60×10^{-15} [a]	4.63×10^{-14} [b]	4.98×10^{-15} [b]

[a] From Ref. 21; [b] From Ref. 22.

Table 2: Variational Γ^{CVT} and tunneling $\kappa^{\mathrm{CVT/SCT}}$ transmission coefficients for the TS-t (conformer 1) and the TS-g^+ (conformer 2) transition states at room temperature. The imaginary frequency at the transition state ($\omega^\star$) and the difference in the vibrationally adiabatic potential (in kcal/mol) between the transition states and the most stable conformation of reactants are also listed.

Reaction	TS conformer	$\omega^\star$	$\Delta V_a^{\ddagger \mathrm{G}}$	Γ^{CVT}	$\kappa^{\mathrm{CVT/SCT}}$
R1	1	$1281i$	4.87	0.994	3.30
	2	$1285i$	5.05	0.987	3.35
R2	1	$981i$	6.01	0.907	3.23
	2	$984i$	6.17	0.894	3.41
R3	1	$1240i$	4.13	0.690	2.59
	2	$1247i$	4.32	0.691	2.57
R4	1	$944i$	5.27	0.998	2.40
	2	$949i$	5.44	0.997	2.50

Table 3: Contribution at room temperature of each of the two transition state conformers to the terms in which the KIE was factorized. The total theoretical and experimental KIEs are also listed.

KIE	TS conformer	η_{tor}	η_{trans}	$\eta^{\ddagger}_{\text{rv}}$	η_{vtun}	$P_{i,\text{D}}$	$\tilde{\eta}_i$	$\tilde{\eta}$	η_{exp}
R1/R2	1	1.001	1.003	6.958	1.120	0.557	4.360	7.66	$7.38^{+0.94\,a}_{-0.85}$
	2	1.001	1.003	6.845	1.095	0.443	3.304		
R1/R3	1	0.999	2.740	0.197	1.832	0.575	0.570	1.00	$0.73^{+0.06\,b}_{-0.05}$
	2	0.999	2.740	0.199	1.861	0.425	0.432		
R1/R4	1	0.997	2.757	1.394	1.369	0.559	2.934	5.16	$6.80^{+1.28\,b}_{-0.98}$
	2	0.997	2.757	1.383	1.327	0.441	2.223		

[a] From Ref. 21; [b] From Ref. 22.

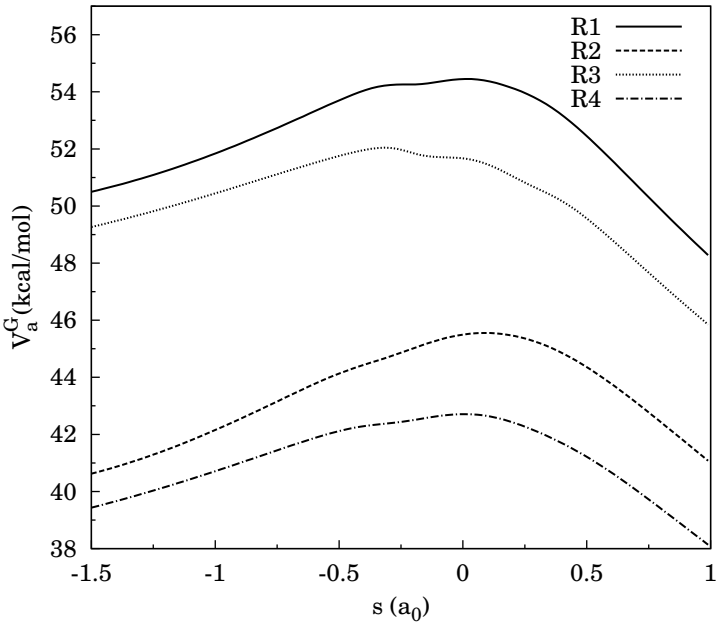

Figure 1: Plot of the vibrationally abiabatic potential, $V_{\rm a}^{\rm G}$ as a function of the reaction coordinate s for reactions R1 to R4 starting from transition state TS-t. The profiles starting from TS-g^+ are similar to the ones of the plot.

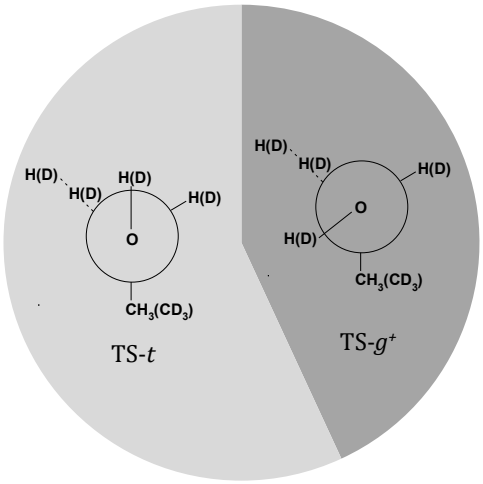

Percentage contribution of each transition to the hydrogen abstraction reaction. This percentage is independent of the isotopic substitution.

ToC